Trop J Nat Prod Res, December 2025; 9(12): 6227 - 6234

ISSN 2616-0684 (Print)
ISSN 2616-0692 (Electronic)

Tropical Journal of Natural Product Research

Available online at https://www.tjnpr.org

Original Research Article

The Employment of FTIR Spectroscopy and Multivariate Data Analysis for Authentication Study of Sacha Inchi Seed Oil

Youstiana D. Rusita[1,2], Abdul Rohman[1]*, Marlyn D. Laksitorini[3], Purwanto Purwanto[4]

[1]*Department of Pharmaceutical Chemistry, Faculty of Pharmacy, Universitas Gadjah Mada, Yogyakarta 55281, Indonesia.*
[2]*Department of Pharmaceutical and Food Analysis, Surakarta Health Polytechnic, Surakarta 57127, Indonesia.*
[3]*Department of Pharmaceutics, Faculty of Pharmacy, Universitas Gadjah Mada, Yogyakarta 55281, Indonesia.*
[4]*Department of Pharmaceutical Biology, Faculty of Pharmacy, Universitas Gadjah Mada, Yogyakarta 55281, Indonesia.*

ARTICLE INFO

Article history:
Received 06 December 2024
Revised 19 November 2025
Accepted 28 November 2025
Published online 01 January 2026

ABSTRACT

Sacha inchi (*Plukenetia volubilis*) is recognized as one of the world's most versatile plants, with nearly all parts suitable for use as food ingredients. Sacha inchi seed oil (SIO) commands a premium price in the online market, approximately tenfold higher than conventional vegetable oils such as palm oil (PO), making it a prime target for economically motivated adulteration. This study aimed to establish a robust analytical approach for the discrimination and quantification of PO and soybean oil (SBO) adulterants in authentic SIO using Fourier Transform Infrared (FTIR) spectroscopy coupled with chemometrics. FTIR spectral data were acquired for pure SIO, PO, SBO, and their mixtures across the mid-infrared range (4000–650 cm^{-1}). Principal component analysis (PCA) of full-spectrum absorbance values revealed spectral proximity between SIO and SBO, indicating potential challenges in visual differentiation. Principal component regression (PCR) applied to selected spectral regions (3010–2830 and 1800–700 cm^{-1}) yielded the highest calibration and prediction performance, with coefficients of determination (R^2) values of 0.9991 and minimal root mean square error of calibration (RMSEC = 0.620) and validation (RMSEP = 0.658). The developed models demonstrated high accuracy and precision, validating the reliability of FTIR-chemometric integration for authenticating SIO and detecting adulteration with lower-cost oils. This approach offers a rapid, non-destructive, and cost-effective solution for quality control in functional oil authentication.

Keywords: Sacha Inchi Seed Oil, Adulteration, Chemometrics, Authentication Analysis, Fourier Transform Infrared.

Introduction

Sacha inchi (*Plukenetia volubilis L.*) is widely recognized as a valuable source of functional food oils. Sacha inchi seed oil (SIO) contains essential unsaturated fatty acids (USFA), including ω-3 fatty acids (notably α-linolenic acid, for approximately 51%) and ω-6 fatty acids (linoleic acid, for approximately 34%). These omega fatty acids are reported to provide beneficial effects to human health, such as protection against cardiovascular disease.[1,2] In addition to fatty acids, SIO also contains minor bioactive components such as polyphenols, carotenoids, and tocopherols, which are believed to contribute to its pharmacological activities, including antioxidant, antidyslipidemic, antitumor, and antiproliferative effects.[3,4] Due to these properties, SIO is increasingly utilized in food, pharmaceutical, and cosmetic formulations. In the fats and oils industry, SIO is expensive due to its nutritional benefits. This economic appeal makes it vulnerable to adulteration by unscrupulous manufacturers, who may substitute SIO wholly or partially with cheaper vegetable oils such as SBO and PO. Although these adulterants are classified as "edible," such practices can pose health risks to consumers. Therefore, the development of reliable detection methods is crucial, not only for regulatory agencies but also for producers and health professionals.

*Corresponding author. Email: abdul_kimfar@ugm.ac.id
Tel: +62 878-3844-5216

Citation: Rusita YD, Rohman A, Laksitorini MD, Purwanto P. The Employment of FTIR Spectroscopy and Multivariate Data Analysis for Authentication Study of Sacha Inchi Seed Oil. Trop J Nat Prod Res. 2025; 9(12): 6227 – 6234 https://doi.org/10.26538/tjnpr/v9i12.41

Official Journal of Natural Product Research Group, Faculty of Pharmacy, University of Benin, Benin City, Nigeria

Given the similar physical appearance between SIO and its adulterants, sophisticated analytical instruments such as spectrometers (IR, Raman, NMR), differential scanning calorimeters, and chromatographs are essential for authentication.[5] Among these, FTIR spectroscopy has emerged as a preferred tool for authenticating high-value edible oils due to its fingerprinting capabilities.[6] FTIR spectroscopy is well-suited for rapid screening, authentication, and quantitative analysis of oil adulterants with minimal sample preparation. When combined with chemometric techniques, such as pattern recognition and multivariate calibration, FTIR has been successfully applied to authenticate premium edible oils, including extra virgin olive oil,[7] virgin coconut oil (VCO),[8] avocado oil,[9] red fruit oil (RFO),[10] ginger oil,[11] and sesame oil.[12] This approach is fast, non-destructive, and requires simple sample preparation.[13] Common multivariate calibration methods include partial least squares regression (PLSR) and PCR, while linear discriminant analysis (LDA) is used to explore relationships between descriptive and categorical variables. This study aims to authenticate SIO adulterated with PO and SBO using FTIR spectroscopy integrated with chemometrics. PLSR and PCR were employed for quantitative analysis, while LDA was used for classification. To the best of our knowledge, this is the first comprehensive investigation combining FTIR spectroscopy with LDA, PLSR, and PCR to simultaneously quantify and classify PO and SBO adulteration in SIO. This integrated analytical framework offers a rapid, non-destructive, and cost-effective solution for authenticating edible oils susceptible to economic adulteration.

Materials and Methods

Materials

Sacha inchi (*Plukenetia volubilis* L.) seeds were harvested from cultivated plots in Sleman (-7.7726, 110.253601), Yogyakarta, Indonesia, between May and August 2024. Taxonomic identification was conducted by the Department of Plant Taxonomy, Semarang State

University, Central Java, Indonesia, and confirmed under voucher number 109/UN.37/SHP/Lab. Plant Taxonomy/VII/2024. Seed authentication and preliminary analysis were performed at the Integrated Laboratory of the Faculty of Mathematics and Natural Sciences, Semarang State University.

A total of eleven commercial vegetable oils, namely PO, corn oil, canola oil, sunflower oil, avocado oil, SBO, mustard oil, olive oil, extra virgin olive oil, VCO, and RFO, were procured from retail outlets in Solo-Yogyakarta. These oils were selected based on their prevalence in the Indonesian market and their potential as adulterants in authenticity studies. All solvents used for FTIR measurements were of analytical grade.

Preparation of Sacha Inchi Seed Oil

SIO was extracted using a cold-press mechanical method, which preserves the native lipid profile and minimizes thermal degradation.[14] This method aligns with protocols described by Kong et al. (2023) who emphasized that cold-pressing preserves the USFA profile and bioactive compounds of SIO.[15] Before extraction, the seeds were hand-peeled to eliminate the outer husk, producing white kernels. The kernels were oven-dried at 60 °C to lower moisture and improve oil recovery. The dried seeds were then pressed using a mechanical cold press, and the resulting oil was filtered to remove particulates. Sodium sulfate (Na_2SO_4, Sigma-Aldrich, Germany) was used to eliminate residual moisture. The purified oil was stored in amber glass bottles at 4°C to prevent oxidative degradation.[16]

FTIR Measurement

FTIR spectra of SIO and reference oils were recorded using a Nicolet 6700 FTIR spectrometer (Thermo Nicolet, Madison, USA) equipped with a deuterated triglycine sulfate (DTGS) detector and KBr beam splitter. Spectra were acquired using a horizontal attenuated total reflectance (HATR) accessory with a ZnSe crystal. Each sample was applied using a Pasteur pipette, and 32 scans were collected per sample at a resolution of 8 cm^{-1} over the mid-infrared range (4000-650 cm^{-1}). Ambient temperature was maintained at 25°C. Spectra were ratioed against a fresh air background and recorded in triplicate to ensure reproducibility.[17] Spectra are available in Supplementary Data A.

Principal component analysis (PCA) of oils

PCA was performed to explore clustering patterns and spectral variance among SIO and the eleven reference oils. The analysis was conducted using Minitab version 17 (Minitab Inc., USA). PCA score plots of the first two principal components (PC1 and PC2) were used to identify oils with spectral profiles similar to SIO, which were considered potential adulterants. The entire mid-infrared region (4000-650 cm^{-1}) was included in the analysis to capture both fingerprint and functional group regions.[18]

Linear discriminant analysis (LDA)

LDA was applied to differentiate authentic SIO from samples adulterated with PO and SBO, which were selected based on their spectral proximity and market prevalence. The classification was performed using TQ Analyst™ version 9 (Thermo Fisher Scientific, Inc.), a chemometric software platform designed for supervised pattern recognition based on spectral data.[19] The LDA model was constructed using a training dataset comprising pure SIO and SIO adulterated with PO and SBO at graded concentrations ranging from 1% to 50% (v/v). Each mixture was prepared under controlled conditions to simulate realistic scenarios of adulteration. FTIR spectra of these samples were collected and preprocessed to ensure baseline correction and normalization before model input. To evaluate model performance, a validation set of independent samples, unseen during training, was introduced. These samples included both pure and adulterated oils at random concentrations within the defined range. The model's classification accuracy was assessed by comparing predicted group membership against true labels, and the percentage of correctly classified samples was recorded as a measure of model robustness. LDA starts with a number of samples whose group membership is known and named with learning or training datasets (one group is authentic SIO and another one is adulterated SIO). Furthermore, the independent samples whose membership is unknown were prepared to test the learning datasets model. SIO and oil adulterants (PO and SBO) were mixed to get a series of training sets of pure SIO and adulterated with PO and SBO in the concentration range of 1-50%. The accuracy of the LDA model was evaluated by the number of independent samples (validation samples) that were correctly misclassified.

Multivariate calibration

Multivariate calibration was employed to quantify the concentration of adulterants in SIO using PLSR and PCR. These regression models were developed based on the FTIR spectral data of pure and adulterated oil samples, enabling the prediction of adulterant levels with high sensitivity and precision. The FTIR dataset was systematically divided into three subsets, namely calibration, validation set, and testing set.[17] PLSR was selected for its ability to handle collinear and high-dimensional spectral data, making it particularly suitable for FTIR-based quantification. PCR was also applied as a comparative method, leveraging PC scores derived from spectral variance to construct regression models. All multivariate analyses were conducted using TQ Analyst™ version 9 (Thermo Fisher Scientific, Inc.), which supports supervised calibration workflows and integrates seamlessly with FTIR spectral inputs. While LDA was used for categorical classification between authentic and adulterated samples, PLSR and PCR provided quantitative estimates of adulterant concentrations across a range of 1-50% (v/v).

Results and Discussion

FTIR spectroscopy is an effective method for identifying chemical structures by correlating each absorbance band with particular functional groups.[20] FTIR spectroscopy is a powerful analytical method for characterizing edible fats and oils, offering excellent specificity in authentication analyses. FTIR improves sample differentiation by collecting unique spectral profiles that reveal changes in absorbance strengths, especially in characteristic peak areas and shoulder features.[21] The distinctive spectral features observed in FTIR measurements can be systematically interpreted using chemometric techniques to achieve precise oil classification, thereby enabling reliable adulteration detection and ensuring the preservation of product authenticity.[20]

Figure 1A shows a score plot of PC1 and PC2 obtained from PCA for the classification of studied oils using absorbance values of FTIR spectra at wavenumbers of 3010-719 cm^{-1}. The PCA score plot identified six discrete categories of edible oils according to their FTIR absorbance profiles (3010-719 cm^{-1}), indicating variations in fatty acid composition and minor constituents: Group I (SIO), Group II (RFO), Group III (corn oil, SBO, mustard oil, canola oil, and olive oil), Group IV (avocado oil), Group V (extra virgin olive oil and PO), and Group VI (VCO). Collectively, these clusters demonstrate how PCA proficiently differentiates oils based on their predominant lipid classes and bioactive constituents. Among the eleven edible oils analyzed, specifically PO, corn oil, canola oil, sunflower oil, avocado oil, SBO, mustard oil, olive oil, extra virgin olive oil, VCO, and RFO; SIO exhibited spectral characteristics and physicochemical properties most closely related to corn oil, SBO, mustard oil, SIO, and olive oil (Group III). This finding confirms prior research indicating that SIO exhibits compositional similarities with olive oil, especially due to the high concentration of USFAs, especially oleic acid, detected in both oils.[22,23] PC1 (81.4%) and PC2 (15.1%) cumulatively explained 96.5% of the total variance, with the highest eigenvector loadings (Figure 1B) observed at 1743 cm^{-1} (- 0.358) for PC1 and 2919 cm^{-1} (- 0.363) for PC2.

To further investigate the separation observed in Group III, the dataset was reanalyzed by excluding the other oil samples, and the resulting PCA score plot is presented in Figure 1C. This refined analysis revealed five distinct clusters: Group I (mustard oil), Group II (olive oil), Group III (canola oil), Group IV (corn oil), and Group V (SBO and sunflower oil). The first two principal components accounted for a substantial proportion of the total variance, with PC1 explaining 44.0% and PC2 explaining 33.9%, together capturing 77.9% of the overall variability in the dataset. The corresponding loading plot (Figure 1D) indicated that the most influential spectral variables were located at 1745 cm^{-1} (0.196)

ISSN 2616-0684 (Print)
ISSN 2616-0692 (Electronic)

for PC1, associated with ester C=O stretching vibrations, and at 968 cm^{-1} (0.227) for PC2, typically linked to out-of-plane =C–H bending in USFA.

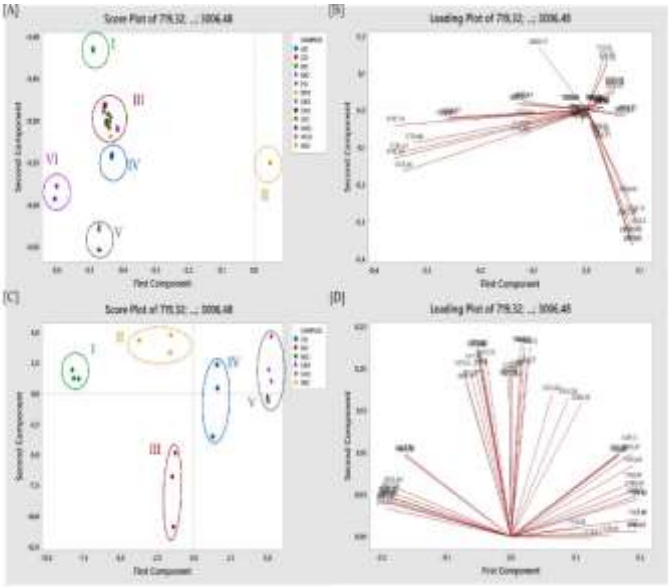

Figure 1: Principal component analysis (PCA) of the dataset. [A] Score plot of all samples, showing six groups (I–VI) separated by their first and second principal components. [B] Corresponding loading plot indicating the variables contributing most strongly to group separation. [C] Score plot of selected samples (groups I–V), highlighting refined clustering patterns. [D] Corresponding loading plot for the selected groups, showing variable contributions to the observed distribution. (AO = Avocado oil, CO = Corn oil, KO = Canola oil, MO = Mustard oil, PO = Palm oil, RFO = Red fruit oil, SBO = Soybean oil, SFO = Sunflower oil, SIO = Sacha inchi seed oil, VCO = Virgin coconut oil, VOO = Virgin olive oil, WO = Olive oil)

Chemically, edible fats and oils, including SIO, PO, and SBO, are primarily composed of triacylglycerols, formed by the esterification of three fatty acids with a glycerol backbone.[24–26] Due to the compositional similarities among these oils, particularly in their USFA profiles, visual detection of adulteration is often unreliable.[27] Due to its unique fingerprinting features, mid-infrared (MIR) spectroscopy is an effective analytical method for differentiating genuine edible oils from adulterated ones. This method may distinguish between authentic oils and those adulterated with others by analyzing spectral changes caused by the adulteration practice.[28]

Figure 2 shows that there were unique spectral bands in the 1120-1000 cm^{-1} range and at 725 cm^{-1}. These bands are characteristic of SIO. The absorption in the 1120-1000 cm^{-1} range was due to the stretching vibrations of C–O bonds in ester groups. These groups are usually found in triacylglycerol complexes that comprise esters made from primary and secondary alcohols. These bands represent the molecular backbone of edible oils and indicate the presence of oxygenated functional groups, which are crucial for identifying oils. Meanwhile, the strong band at 725 cm^{-1}, on the other hand, was attributed to the rocking vibrations of methylene (–CH_2–) groups, which are the same as the out-of-plane bending vibrations of cis-disubstituted olefinic moieties. These spectra were especially useful for figuring out the structures of USFAs like oleic and linoleic acids, which are common in SIO and contribute to its nutritional and chemical composition.[25,29–31] These bands represent the molecular composition of edible oils and indicate the presence of oxygenated functional groups essential for oil authenticity.

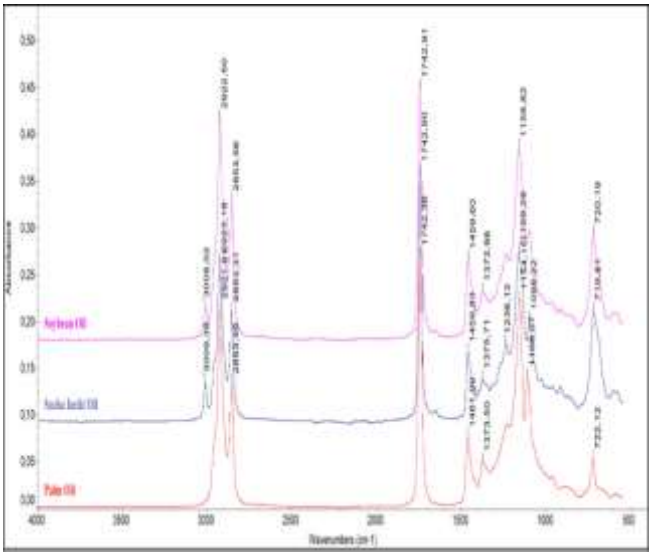

Figure 2: FTIR spectra of PO, SBO, and SIO at wavenumbers of 3500–400 cm^{-1}

Table 1 illustrates the assignment of each functional group that constitutes SIO as identified through FTIR spectroscopy. The stretching vibration of the cis-olefinic =CH was observed at 3008-3009 cm^{-1} (3010 cm^{-1} in the refined sample); the elevated frequency of this band signifies the abundance of polyunsaturated acyl groups (PAG). Among the various oils examined in this study, SIO exhibited the highest methylene stretching band at 2923 cm^{-1}, surpassing those observed in SBO (2922 cm^{-1}) and PO (2921 cm^{-1}).

Table 1: Compilation of the wavenumbers of each peak and shoulders in FTIR spectra of SIO, SBO, and PO, and the corresponding functional groups' vibration (38)(33)(34)

Wavenumber (cm^{-1})	Type of Bending and Vibration
3008	C=CH Stretching
2923 – 2850	-$CH(CH_3)$ Stretching Asymmetric
1742	–C=O (ester) Stretching
1450 – 1465	–CH_2 bending
1372-1373	Symmetrical bending vibrations of the CH_3 groups
1227 – 1230	stretching vibration of the C–O ester
1158 – 1160	–C–O stretch; –CH_2 bending
720 - 721	cis-CH=CH– bending out of plane
965	trans–CH=CH–Bending out of plane
914	trans–CH=CH–Bending out of plane
721	cis-CH=CH– bending out of plane

The two bands resulting from the methylene asymmetrical and symmetrical stretching vibrations appear at 2927 cm^{-1} and 2855 cm^{-1}.[32] The peak at 1742 cm^{-1} corresponds to the –C=O stretch, which was one of the lowest observed in vegetable oils and was characteristic of oils with a high degree of USFAs. The peak at 1461 cm^{-1} is associated with –CH_2 bending, and the peak at 1417 cm^{-1} is attributed to cis =C–H bending vibration. When compared to the spectral profiles and compositional parameters of other vegetable oils, the elevated absorbance values in specific regions of the FTIR spectrum suggest a pronounced level of unsaturation in the analyzed oil sample. It is indicative of a high concentration of mono- and polyunsaturated fatty acids (PUFA), which is consistent with the chemical characteristics of oils rich in oleic and linoleic acids.[21,25,33] The absorption band observed at 1376 cm^{-1} was attributed to –CH_3 bending vibration, while the peak at 1236 cm^{-1} was associated with C–O stretching vibration, and the

ISSN 2616-0684 (Print)
ISSN 2616-0692 (Electronic)

prominent peak at 1160 cm^{-1} was due to the C–O stretching and CH_2 bending ascribed to ester functionalities and methylene group vibrations, displaying negligible change among various vegetable oils. Conversely, the observed band between 1096^{-1} and 1100 cm^{-1}, indicating the vibration of C–O stretching, has a more robust association with the relative quantity of monounsaturated and PAG chains in the oil composition.

Moreover, the absorption at 965 cm^{-1}, attributed to trans-CH=CH out-of-plane bending, acts as a dependable measure of unsaturation levels. Comparative data from pure triacylglycerols indicate that tristearin, tripalmitin, trilinolenin, and trilinolein display bands at 920 cm^{-1}, 916 cm^{-1}, 915 cm^{-1}, and 914 cm^{-1}, respectively. However, triolein exhibits a weak shoulder at 904 cm^{-1}, rather than a distinct peak in the SIO spectra, which can be considered typical of an oil sample rich in the PAGs, and the peak observed at 721 cm^{-1} corresponds to cis–CH=CH– bending out-of-plane vibration.[32,34] The presence of a distinct peak at 965 cm^{-1} in the FTIR spectrum of SIO indicates a significant concentration of PUFAs [32].

Figure 1 illustrates that SIO can be differentiated from other edible oils primarily by the fingerprint area (1500–650 cm^{-1}), as confirmed by PCA results. Based on the FTIR spectrum examination of SIO, SBO, and PO, it was revealed that the spectral profile of SIO exhibits greater similarity to SBO than to PO, particularly in significant vibrational regions, as can be seen in Figure 1. Therefore, implementing multivariate classification models based on targeted spectral regions is essential for verifying the authenticity of SIOs and, when applicable, quantifying the extent of their adulteration with PO and SBO vegetable oils.

Quantification of Oil Adulterants (PO and SBO) in SIO

Multivariate calibration models, notably PLSR and PCR, were utilized to estimate the presence of PO and SBO as adulterants in SIO. These chemometric methods are esteemed for being successful in controlling sophisticated spectroscopic datasets and for facilitating accurate predictions of chemical concentrations based on spectral fluctuations. PLSR and PCR integrate spectral data (X variables) and concentration values (Y variables) into a single analytical framework, facilitating simultaneous dimensionality reduction and model optimization. This method enables multivariate calibration in quantifying PO and SBO as adulterants in SIO through allowing simultaneous data analysis within modeling frameworks using PLSR and PCR algorithms.[35]

The spectral regions used in PLSR and PCR calibration models are subjected to optimization. Finally, the absorbance values at combined wavenumbers of 1800-1600 and 980-700 cm^{-1} were selected for quantitative analysis for SBO in SIO (Table 2), and at combined wavenumbers of 3010-2830 cm^{-1} and 1800-800 cm^{-1} for quantification of PO in SIO (Table 3).

Table 2: The performance of multivariate calibrations for quantitative analysis of SBO as an adulterant in SIO (The bolded item shows the selected criteria)

Wave number (cm^{-1})	Multivariate Calibration	Spectra	Factor (PC)	R^2		RMSEC	RMSEP	RMSEP/ RMSEC
				Calibration	Validation			
1800-1200	PLS	Normal	4	0.9956	0.9809	1.410	3.060	2.17
		1st Derivative	3	0.9968	0.9928	1.200	1.880	1.57
		2nd Derivative	4	0.9964	0.9913	1.270	2.110	1.66
	PCR	Normal	8	0.9990	0.9987	0.656	0.983	1.50
		1st Derivative	8	0.9975	0.9959	1.060	1.420	1.34
		2nd Derivative	8	0.9960	0.9933	1.340	1.840	1.37
1100-700	PLS	Normal	3	0.9979	0.9988	0.968	0.810	0.84
		1st Derivative	2	0.9981	0.9987	0.937	0.879	0.94
		2nd Derivative	3	0.9968	0.9960	1.200	1.440	1.20
	PCR	Normal	10	0.9986	0.9991	0.785	0.686	0.87
		1st Derivative	10	0.9987	0.9991	0.780	0.713	0.91
		2nd Derivative	10	0.9956	0.9955	1.400	1.630	1.16
1800 - 700	PLS	Normal	4	0.9985	0.9984	0.743	0.895	1.20
		1st Derivative	6	0.9991	0.9991	0.589	0.745	1.26
		2nd Derivative	6	0.9993	0.9991	0.533	0.743	1.39
	PCR	Normal	4	0.9991	0.9989	0.645	0.731	1.13
		1st Derivative	4	0.9990	0.9990	0.681	0.679	1.00
		2nd Derivative	4	0.9976	0.9977	1.020	1.050	1.03
3010 – 2830 and 1800 - 700	PLS	Normal	5	0.9986	0.9985	0.732	0.892	1.22
		1st Derivative	5	0.9985	0.9986	0.745	0.875	1.17
		2nd Derivative	5	0.9987	0.9987	0.707	0.842	1.19
	PCR	**Normal**	**8**	**0.9993**	**0.9995**	**0.546**	**0.481**	**0.88**
		1st Derivative	8	0.9987	0.9988	0.772	0.882	1.14
		2nd Derivative	8	0.9985	0.9984	0.825	0.909	1.10
1800-1600 and 980-700	PLS	Normal	2	0.9768	0.9882	3.220	2.480	0.77
		1st Derivative	4	0.9992	0.9990	0.617	0.790	1.28
		2nd Derivative	5	0.9971	0.9889	1.150	2.240	1.95
	PCR	Normal	10	0.9992	0.9987	0.604	0.823	1.36
		1st Derivative	10	0.9989	0.9989	0.689	0.825	1.20
		2nd Derivative	10	0.9942	0.9862	1.610	2.680	1.66

ISSN 2616-0684 (Print)
ISSN 2616-0692 (Electronic)

Table 3: The performance of multivariate calibrations for quantitative analysis of PO as an adulterant in SIO (The bolded item shows the selected criteria)

Wave number (cm^{-1})	Multivariate Calibration	Spectra	Factor (PC)	R^2		RMSEC	RMSEP	RMSEP/ RMSEC
				Calibration	Validation			
1800-1200	PLS	Normal	6	0.9990	0.9985	0.629	0.859	1.37
		1st Derivative	6	0.9988	0.9985	0.679	0.879	1.29
		2nd Derivative	8	0.9993	0.9990	0.530	0.701	1.32
	PCR	Normal	5	0.9965	0.9940	1.150	1.670	1.45
		1st Derivative	5	0.9946	0.9899	1.430	2.150	1.50
		2nd Derivative	5	0.9949	0.9897	1.390	2.170	1.56
1100-700	PLS	Normal	3	0.9986	0.9982	0.733	0.983	1.34
		1st Derivative	4	0.9989	0.9986	0.633	0.882	1.39
		2nd Derivative	1	0.9971	0.9970	1.060	1.200	1.13
	PCR	Normal	6	0.9989	0.9988	0.659	0.839	1.27
		1st Derivative	6	0.9984	0.9988	0.780	0.804	1.03
		2nd Derivative	6	0.9976	0.9978	0.963	1.040	1.08
1800 - 700	PLS	Normal	4	0.9985	0.9984	0.743	0.895	1.20
		1st Derivative	6	0.9991	0.9991	0.589	0.745	1.26
		2nd Derivative	6	0.9993	0.9991	0.533	0.743	1.39
	PCR	Normal	4	0.9991	0.9989	0.645	0.731	1.13
		1st Derivative	4	0.9990	0.9990	0.681	0.679	1.00
		2nd Derivative	4	0.9976	0.9977	1.020	1.050	1.03
3010 – 2830 and 1800 - 700	PLS	Normal	5	0.9986	0.9985	0.732	0.892	1.22
		1st Derivative	5	0.9985	0.9986	0.745	0.875	1.17
		2nd Derivative	5	0.9987	0.9987	0.707	0.842	1.19
	PCR	**Normal**	**4**	**0.9991**	**0.9992**	**0.620**	**0.658**	**1.06**
		1st Derivative	4	0.9962	0.9956	1.290	1.500	1.16
		2nd Derivative	4	0.9789	0.9737	3.040	3.690	1.21
1800-1600 and 980-700	PLS	Normal	3	0.9988	0.9982	0.677	0.967	1.43
		1st Derivative	6	0.9994	0.9988	0.461	0.360	0.78
		2nd Derivative	6	0.9993	0.9978	0.507	1.080	2.13
	PCR	Normal	6	0.9990	0.9987	0.622	0.857	1.38
		1st Derivative	6	0.9988	0.9983	0.671	0.937	1.40
		2nd Derivative	6	0.9977	0.9952	0.938	1.560	1.66

The results obtained from PLS and PCR models in terms of R^2, RMSEC, and RMSEP for either the normal spectra and its derivatives (the first derivative and second derivative) for the authentication study of SIO with SBO and PO can be seen in Tables 2 and 3, respectively.

Tables 2 and 3 compile the predictive performance of FTIR spectroscopy across different wavenumber intervals and spectral treatments, combined with multivariate calibration, for estimating SIO levels adulterated with SBO (Table 2) and PO (Table 3). PCR on unprocessed FTIR spectra within 3010-2830 cm^{-1} and 1800-700 cm^{-1} was selected for quantifying SIO in PO, as it achieved the highest R^2 (0.9991) in both calibration and prediction alongside the minimal RMSEC (0.620) and RMSEP (0.658). According to Zhan et al (2017). a reliable model should have low RMSEC, RMSECV, and RMSEP values with little variation between RMSECV and RMSEP.[36] Additionally, both the PO and SBO models in this study met the criteria that RMSEP should not be greater than 1.2 times the RMSEC. These results support the applicability of this technique in routine quality control and regulatory settings and are consistent with earlier research on edible oil authentication using FTIR–chemometric approaches.[37–39] Using FTIR spectroscopy in conjunction with multivariate calibration is a statistically viable and effective technique for quantifying oil adulteration.

Using calibration and validation models across a range of wavenumber regions and FTIR spectral treatments, the effectiveness of PLS for the quantitative analysis of SIO in binary mixtures with PO was assessed. Based on their ability to generate the highest R^2 between actual and predicted SIO concentrations and the lowest error values, as shown by the RMSEC and RMSEP, the modeling conditions were chosen. A key indicator of model accuracy is the R^2 values, where higher values indicate better predictive reliability. R^2 was used as the primary indicator of model accuracy, with larger values reflecting greater predictive reliability

The error of calibration models was evaluated using RMSEC,[40] calculated as equation 1:

$$RMSEC = \sqrt{\frac{\sum_{i=1}^{n}(actual-caltulated)^2}{N-f-1}} \quad \text{.....(1)}$$

"Actual value" denotes the certified concentration of the standard, while "predicted value" (or "calculated value") is the concentration estimated by the FTIR-based model. N represents the number of samples in the calibration set and f denotes the number of factors in the calibration model. Lower RMSEC indicates better model performance. In this study, RMSEC values were 0.620 for PO (Figure 3A) and 0.546 (Figure 3B) for SBO, reflecting high calibration accuracy.

PLSR was employed to quantify the concentration of PO and SBO in SIO samples to evaluate the prediction capability of the calibration model. Two significant statistical metrics were employed to assess the model's performance: the RMSEP, which quantifies the difference between the predicted and actual values in the validation set, and the R^2, which indicates the goodness of fit. RMSEP[40] was calculated as equation 2:

$$RMSEP = \sqrt{\frac{\sum_{i=1}^{n}(actual-caltulated)^2}{M-1}} \quad \text{.....(2)}$$

M denotes the number of samples in the prediction set. Figure 5 revealed that R^2 values in validation models are 0.9991 and 0.9993 for PO and SBO, respectively. The RMSEP values for PO and SO as adulterants in SIO samples are 0.658 and 0.481, respectively. These findings demonstrate that the combination of FTIR spectral data with multivariate calibration techniques, specifically PLS and PCR, provides a reliable and effective approach for quantifying the levels of PO and SBO as adulterants in SIO. The predictive accuracy of the developed models is supported by high R^2 in both calibration and validation phases. At the same time, the low RMSEC and RMSEP values confirm the precision and robustness of the analytical framework.

ISSN 2616-0684 (Print)
ISSN 2616-0692 (Electronic)

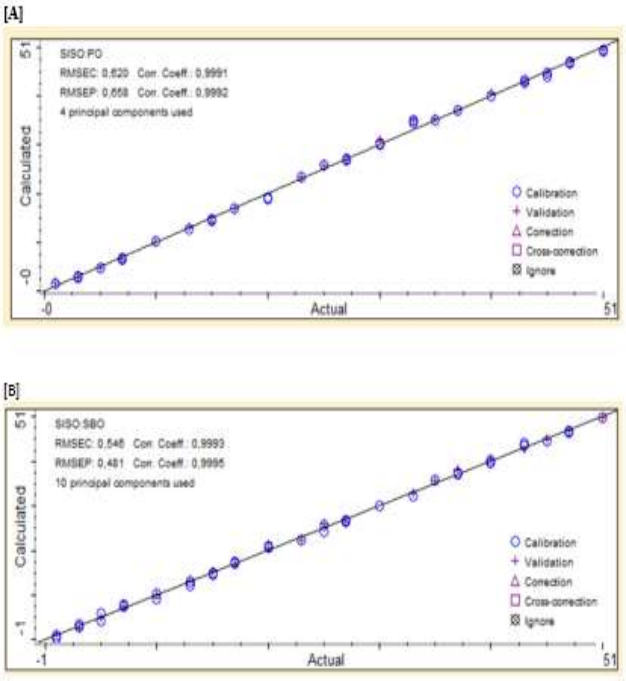

Figure 3: The relationship between actual values (x-axis) of SIO in PO and SBO and the predicted values of SIO using FTIR spectroscopy [A and B].

Classification of authentic SIO adulterated with PO and SIO adulterated with SBO

LDA, a supervised pattern recognition technique, was employed to classify SIO samples adulterated with PO and those adulterated with SBO. This method is widely recognized for its effectiveness in distinguishing between predefined classes based on spectral or compositional features. In this current study, LDA was used to create classification models that distinguish genuine SIO from its contaminated variants, thereby enhancing the authentication process through statistically robust discrimination.[41] The variables used for quantitative analysis were also utilized in the LDA to classify SIO samples that were adulterated with PO and SBO. Cooman's plots were created using Mahalanobis distances, which were obtained from the corresponding absorbance values. The classification models successfully distinguished between authentic SIO and its adulterated counterparts with 100% accuracy, as shown in Figures 4 and 5, without any instances of misclassification.[42]

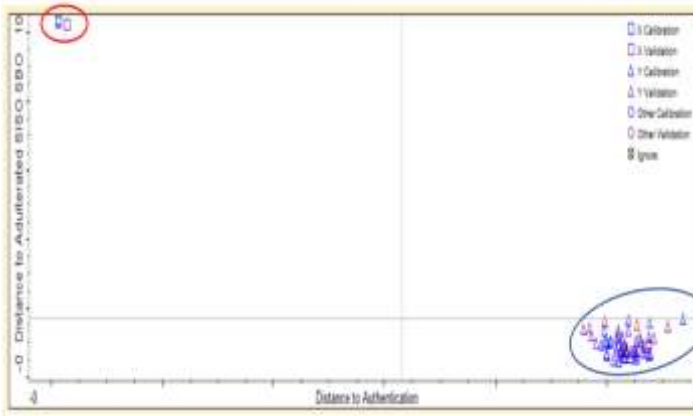

Figure 4: The Cooman's plot was obtained during discriminant analysis for the discrimination of SIO and SIO mixed with SBO

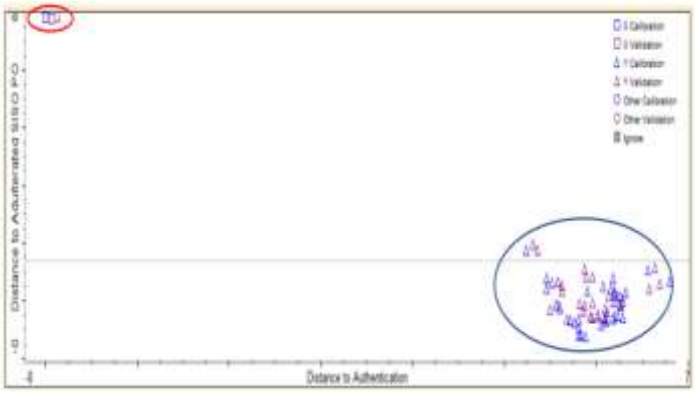

Figure 5: The Cooman's plot was obtained during discriminant analysis for the discrimination of SIO and SIO mixed with PO

Conclusion

FTIR spectroscopy, in combination with multivariate calibration of PCR, was capable of quantifying the levels of SIO adulterated with PO and SIO adulterated with SBO at optimized wavenumbers of 3010-2830 cm^{-1} and 1800-700 cm^{-1}. The model was validated by satisfactory accuracy and precision, evidenced by a high R^2 and low RMSEC and RMSEP. LDA was also successful (100%) for the classification of SIO and SIO adulterated with PO and, SIO and SIO adulterated with SBO. The developed method is rapid and effective for the authentication study of SIO from SBO and PO. Future investigations should concentrate on verifying the approach under commercial-scale circumstances and across various sample matrices to improve industrial applicability and regulatory acceptance. Collaboration with alternative spectroscopic techniques, including spectrofluorometry and near-infrared spectroscopy, in conjunction with artificial intelligence models such as support vector machines and artificial neural networks, could provide scalable, high-throughput solutions for routine authentication and quality control.

Conflict of Interest

The authors declare no conflict of interest.

Authors' Declaration

The authors hereby declare that the work presented in this article is original and that any liability for claims relating to the content of this article will be borne by them.

Acknowledgements

The authors would like to express their sincere gratitude to Dr. Djoko Santosa for his invaluable supervision and guidance throughout the determination of sacha inchi (*Plukenetia volubilis L.*) plant, which was conducted at the Department of Pharmaceutical Biology. We also extend our appreciation to the Director of Surakarta Health Polytechnic for the institutional support for this study.

References

1. Cárdenas DM, Rave LJG, Soto JA. Biological activity of Sacha Inchi (*Plukenetia volubilis* Linneo) and potential uses in human health: A review. Univ Zagreb. 2021; https://doi.org/10.17113/ftb.59.03.21.6683
2. Samrit T, Osotprasit S, Chaiwichien A, Suksomboon P, Chansap S. Cold-pressed Sacha Inchi oil: High in omega-3 and prevents fat accumulation in the liver. 2024.
3. Mhd Rodzi NAR, Lee LK. Sacha Inchi (*Plukenetia volubilis* L.): Recent insight on phytochemistry, pharmacology, organoleptic, safety and toxicity perspectives. Heliyon. 2022; https://doi.org/10.1016/j.heliyon.2022.e10572
4. Wang S, Zhu F, Kakuda Y. Sacha Inchi (*Plukenetia volubilis* L.): Nutritional composition, biological activity, and uses.

Food Chem. 2018; 265:316–328. https://doi.org/10.1016/j.foodchem.2018.05.055
5. Sudhakar A, Chakraborty SK, Mahanti NK, Varghese C. Advanced techniques in edible oil authentication: A systematic review and critical analysis. Crit Rev Food Sci Nutr. 2023; https://doi.org/10.1080/10408398.2021.1956424
6. Rohman A, Man YBC. Application of Fourier transform infrared spectroscopy for authentication of functional food oils. Appl Spectrosc Rev. 2012; 47(1):1–13. https://doi.org/10.1080/05704928.2011.619020
7. Filoda PF, Fetter LF, Fornasier F, Schneider R de C de S, Helfer GA, Tischer B, Teichmann A, da Costa AB. Fast methodology for identification of olive oil adulterated with a mix of different vegetable oils. Food Anal Methods. 2019; 12(1):293–304. https://doi.org/10.1007/s12161-018-1360-5
8. Rohman A, Che Man YB. The use of Fourier transform mid infrared (FT-MIR) spectroscopy for detection and quantification of adulteration in virgin coconut oil. Food Chem. 2011; 129(2):583–588. https://doi.org/10.1016/j.foodchem.2011.04.070
9. Quiñones-Islas N, Meza-Márquez OG, Osorio-Revilla G, Gallardo-Velazquez T. Detection of adulterants in avocado oil by Mid-FTIR spectroscopy and multivariate analysis. Food Res Int. 2013; 51(1):148–154. https://doi.org/10.1016/j.foodres.2012.11.037
10. Rohman A, Riyanto S, Sasi AM, Yusof FM. The use of FTIR spectroscopy in combination with chemometrics for the authentication of red fruit (Pandanus conoideus Lam) oil from sunflower and palm oils. Food Biosci. 2014; 7:64–70. https://doi.org/10.1016/j.fbio.2014.05.007
11. Syafri S, Hafiz A, Syofyan S, Alen Y, Hamidi D. FT-IR fingerprinting analysis for classification of west sumatra small ginger (*Zingiber officinale* Roscoe) essential oil and its antioxidant activity. Trop J Nat Prod Res. 2024; 8: 6081–6086.
12. Rohman A, Che Man YB. Authentication of extra virgin olive oil from sesame oil using FTIR spectroscopy and gas chromatography. Int J Food Prop. 2012; 15(6):1309–1318. https://doi.org/10.1080/10942912.2010.521607
13. Maggio RM, Kaufman TS, Del Carlo M, Cerretani L, Bendini A, Cichelli A, Compagnone D. Monitoring of fatty acid composition in virgin olive oil by Fourier transformed infrared spectroscopy coupled with partial least squares. Food Chem. 2009; 114(4):1549–1554. https://doi.org/10.1016/j.foodchem.2008.11.029
14. Muangrat R, Veeraphong P, Chantee N. Screw press extraction of Sacha Inchi seeds: Oil yield and its chemical composition and antioxidant properties. J Food Process Preserv. 2018; 42(6) e13635. https://doi.org/10.1111/jfpp.13635
15. Kong S, Keang T, Bunthan M, Say M, Nat Y, Tan CP, Tan R. Hydraulic cold-pressed extraction of Sacha Inchi seeds: Oil yield and its physicochemical properties. ChemEngineering. 2023; 7(4). https://doi.org/10.3390/chemengineering7040069
16. Falodun A, Siraj R, Choudhary MI. GC-MS analysis of insecticidal leaf essential oil of *Pyrenacantha staudtii* Hutch and Dalz (Icacinaceae). Trop J Pharm Res. 2009;8(2):139–143. https://doi.org/10.4314/tjpr.v8i2.44522
17. Khudzaifi M, Retno SS, Rohman A. The employment of FTIR spectroscopy and chemometrics for authentication of essential oil of *Curcuma mangga* from candle nut oil. Food Res. 2020; 4(2):515–521. https://doi.org/10.26656/fr.2017.4(2).313
18. Che Man YB, Rohman A, Mansor TST. Differentiation of lard from other edible fats and oils by means of Fourier transform infrared spectroscopy and chemometrics. J Am Oil Chem Soc. 2011; 88(2):187–192. https://doi.org/10.1007/s11746-010-1659-x
19. Brereton RG. Pattern recognition in chemometrics. Chemom Intell Lab Syst. 2015; 149:90–96. https://doi.org/10.1016/j.chemolab.2015.06.012
20. Rozali NL, Azizan KA, Singh R, Syed Jaafar SN, Othman A, Weckwerth W, Ramli US. Fourier transform infrared (FTIR) spectroscopy approach combined with discriminant analysis and prediction model for crude palm oil authentication of different geographical and temporal origins. Food Control. 2023; 146:109509. https://doi.org/10.1016/j.foodcont.2022.109509
21. Irnawati, Rohman A, Yamin, Fadzillah NA, Azmi AA, Nurlatifah, Windarsih A, Susidarti RA, Ruslin. *Moringa oleifera* seed oils: Physico-chemical characterization and its authentication using FTIR spectroscopy and chemometrics. Case Stud Chem Environ Eng. 2024; 10:100994. https://doi.org/10.1016/j.cscee.2024.100994
22. Faisal MI, Iqbal S, Basra SMA, Afzal I, Saddiq MS, Bakhtavar MA, Hafeez MB. *Moringa* landraces of Pakistan are potential source of premium quality oil. S Afr J Bot. 2020; 129:397–403. https://doi.org/10.1016/j.sajb.2019.10.002
23. Wabaidur SM, AlAmmari A, Aqel A, AL-Tamrah SA, Alothman ZA, Ahmed AYBH. Determination of free fatty acids in olive oils by UPHLC–MS. J Chromatogr B Analyt Technol Biomed Life Sci. 2016; 1031:109–115. https://doi.org/10.1016/j.jchromb.2016.07.040
24. Rigano F, Vento F, Cafarella C, Trovato E, Trozzi A, Dugo P, Mondello L. Determination of main lipids and volatile compounds in unconventional cold-pressed seed oils through chromatographic techniques. J Food Sci. 2025; 90(1):1–17. https://doi.org/10.1111/1750-3841.17661
25. Meng X, Yin C, Yuan L, Zhang Y, Ju Y, Xin K, Chen W, Lv K, Hu L. Rapid detection of adulteration of olive oil with soybean oil combined with chemometrics by Fourier transform infrared, visible-near-infrared and excitation-emission matrix fluorescence spectroscopy: A comparative study. Food Chem. 2023; 405:134828. https://doi.org/10.1016/j.foodchem.2022.134828
26. Sabahannur S, Alimuddin S. Identification of fatty acids in virgin coconut oil (VCO), cocoa beans, crude palm oil (CPO), and palm kernel beans using gas chromatography. IOP Conf Ser Earth Environ Sci. 2022; 1083(1). https://doi.org/10.1088/1755-1315/1083/1/012036
27. Hristy AAC, Asemsumran SK, Yiping DU, Zaki YO. The detection and quantification of adulteration in olive oil by near-infrared spectroscopy and chemometrics. Anal Sci. 2004; 20(June): 935–940.
28. Yap KY, Yung S, Lim CS. Infrared-based protocol for the identification and categorization of ginseng and its products. Food Res Int. 2007; 40(5):643–652. https://doi.org/10.1016/j.foodres.2006.11.009
29. Yang H, Irudayaraj J. Characterization of semisolid fats and edible oils by Fourier transform infrared photoacoustic spectroscopy. J Am Oil Chem Soc. 2000; 77(3):291–295. https://doi.org/10.1007/s11746-000-0048-y
30. Maurer NE, Hatta-Sakoda B, Pascual-Chagman G, Rodriguez-Saona LE. Characterization and authentication of a novel vegetable source of omega-3 fatty acids, Sacha Inchi (*Plukenetia volubilis* L.) oil. Food Chem. 2012; 134(2):1173–1180. https://doi.org/10.1016/j.foodchem.2012.02.143
31. Fahmi Z, Mudasir, Rohman A. Attenuated total reflectance-FTIR spectra combined with multivariate calibration and discrimination analysis for analysis of patchouli oil adulteration. Indones J Chem. 2020; 20(1):1–8. https://doi.org/10.22146/ijc.36955 .
32. Guillén MD, Ruiza A, Caboa N, Chirinosb R, Pascualb G. Characterization of Sacha Inchi (*Plukenetia volubilis* L.) oil by FTIR spectroscopy and 1H NMR. Comparison with linseed oil. J Am Oil Chem Soc. 2003; 80(8):755–762.

33. Arslan FN, Akin G, Karuk Elmas ŞN, Yilmaz I, Janssen HG, Kenar A. Rapid detection of authenticity and adulteration of cold pressed black cumin seed oil: A comparative study of ATR–FTIR spectroscopy and synchronous fluorescence with multivariate data analysis. Food Control. 2019; 98:323–332. https://doi.org/10.1016/j.foodcont.2018.11.055
34. Guillén MD, Cabo N. Characterization of edible oils and lard by Fourier transform infrared spectroscopy. Relationships between composition and frequency of concrete bands in the fingerprint region. J Am Oil Chem Soc. 1997; 74(10):1281–1286. https://doi.org/10.1007/s11746-997-0058-4
35. Rohman A, Ghazali MAB, Windarsih A, Irnawati, Riyanto S, Yusof FM, Mustafa S. Comprehensive review on application of FTIR spectroscopy coupled with chemometrics for authentication analysis of fats and oils in the food products. Molecules. 2020; 25(22):5485. https://doi.org/10.3390/molecules25225485
36. Zhan H, Fang J, Tang L, Yang H, Li H, Wang Z, Yang B, Wu H, Fu M. Application of near-infrared spectroscopy for the rapid quality assessment of *Radix Paeoniae Rubra*. Spectrochim Acta A Mol Biomol Spectrosc. 2017; 183:75–83. https://doi.org/10.1016/j.saa.2017.04.034
37. Riyanta A, Riyanto S, Lukitaningsih E, Rohman A. The employment of Fourier transform infrared spectroscopy (FTIR) and chemometrics for analysis of candlenut oil in Pharm. 2019; 11(2):259–263. https://doi.org/10.22159/ijap.2019v11i2.31758
binary mixture with grape seed oil. Food Res. 2020; 4(1):184–190. https://doi.org/10.26656/fr.2017.4(1).279
38. Putri AR, Aliaño-González MJ, Ferreiro M, Setyaningsih W, Rohman A, Riyanto S, Palma M. Development of a methodology based on headspace-gas chromatography-ion mobility spectrometry for the rapid detection and determination of patin fish oil adulterated with palm oil. Arab J Chem. 2020; 13(10):7524–7532. https://doi.org/10.1016/j.arabjc.2020.08.026
39. Rohman A, Che Man YB, Eakub Ali MD. The authentication of virgin coconut oil from grape seed oil and soybean oil using FTIR spectroscopy and chemometrics. Int J Appl Paradkar MM, Irudayaraj J. A rapid FTIR spectroscopic method for estimation of caffeine in soft drinks and total methylxanthines in tea and coffee. 2002.
40. Rohman A, Che Man YB, Mohd Yusof F. The use of FTIR spectroscopy and chemometrics for rapid authentication of extra virgin olive oil. J Am Oil Chem Soc. 2014; 91(2):207–213. https://doi.org/10.1007/s11746-013-2370-5
41. Fernando D, Permatasari DAI, Hastuti AAMB, Rohman A. Authentication of avocado oil mixed with cooking oils (branded and loose palm oil) utilizing Fourier transform infrared spectroscopy in conjunction with chemometrics. Measurement: Food. 2025; 19. https://doi.org/10.1016/j.meafoo.2025.100241